JOURNAL OF CATALYSIS **169,** 275–286 (1997)
ARTICLE NO. CA971674

Enantioselective Hydrogenation of Ketopantolactone

M. Schürch,* O. Schwalm,*,† T. Mallat,* J. Weber,† and A. Baiker[1,*]

*Department of Chemical Engineering and Industrial Chemistry, ETH Zentrum, CH-8092 Zürich, Switzerland; and †Departement of Physical Chemistry, University of Geneva, 30 quai Ernest-Ansermet, CH-1211 Geneva 4, Switzerland

Received September 4, 1996; revised February 10, 1997; accepted February 24, 1997

The enantioselective hydrogenation of ketopantolactone to *R*-(−)-pantolactone was investigated on 5 wt% Pt/Al_2O_3 chirally modified with cinchonidine. The influence of catalyst pretreatment conditions, hydrogen pressure, temperature, solvent polarity, and catalyst, reactant, and modifier concentrations was studied in a slurry reactor. An enantiomeric excess (ee) of 79% at full conversion was achieved in toluene after optimization of pressure, temperature, and amount of modifier. Good ee could be obtained only after rigorous removal of traces of oxygen and water during catalyst pretreatment and from the hydrogenation reaction mixture. Molecular modeling studies (performed using molecular mechanics, semiempirical, and *ab initio* methods) provided a feasible structure for the diastereomeric transition complex formed between cinchonidine and ketopantolactone and an explanation for the observed enantiodifferentiation in apolar medium. The calculations indicate that formation of the complex affording *R*-(−)-pantolactone is energetically favored with cinchonidine, whereas the near enantiomer cinchonine favors *S*-pantolactone, in agreement with experimental observations. Interestingly, in apolar solvents, where the alkaloid modifier is not protonated, the modeling suggests similar structures for the diastereomeric transition complexes for the hydrogenation of ketopantolactone and methyl pyruvate.

INTRODUCTION

In the past few years the heterogeneous enantioselective hydrogenation of α-ketoesters has become a field of considerable interest for several research groups. The most studied reaction is the hydrogenation of ethyl and methyl pyruvate over supported Pt catalysts modified with cinchona alkaloids (1–6), some other alkaloids (7), or simple chiral N compounds (8–11). Only a few investigations have been made with other α-ketoesters such as methyl benzoylformate (12) and ethyl 4-phenyl-2-oxobutyrate (13).

The enantioselective hydrogenation of ketopantolactone (KPL, dihydro-4,4-dimethyl-2,3-furandione) to *R*-(−)-pantolactone (PL, 2-hydroxy-3,3-dimethyl-γ-butyrolactone) is an industrially important process (Scheme 1). PL is a key intermediate in the synthesis of pantothenic acid (14). In KPL the keto carbonyl group is activated by an ester group in α-position, a structure similar to that of the most studied α-ketoesters. A heterogeneous catalytic method for the production of PL was patented almost a decade ago (15), but the best enantiomeric excess (ee) of 52% with a cinchonidine-modified Pt/C system is far below the accessible values of up to 95% ee for ethyl pyruvate hydrogenation (13).

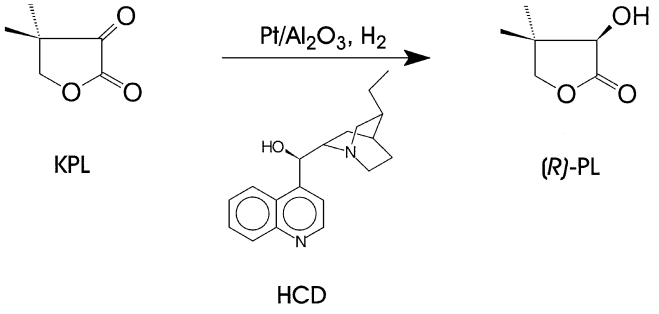

SCHEME 1

The homogeneous catalytic route has attracted more interest in the past. Various rhodium and ruthenium complexes (16–22) have been successfully tested as catalysts in this hydrogenation reaction with ee's up to 99% under very mild conditions (20).

To obtain more information about this important and interesting reaction and to broaden our general knowledge on heterogeneously catalyzed enantioselective reactions, we reinvestigated this reaction using a cinchona-modified Pt/alumina catalyst.

EXPERIMENTAL

10,11-Dihydrocinchonidine (HCD) (Scheme 1) was obtained by hydrogenation under atmospheric pressure of cinchonidine (CD, 98% Fluka) in dilute aqueous HCl over a 5 wt% Pd/alumina catalyst. Under standard conditions, ketopantolactone (KPL, 97% Aldrich) was dissolved in toluene (Fluka) and dried by azeotropic distillation before each reaction. A 5 wt% Pt/alumina catalyst (Engelhard 4759) was used for all experiments. The metal dispersion after heat treatment was 0.27 as calculated from the TEM images (23).

[1] To whom correspondence should be addressed. Fax: (+41-1) 632 11 63.

0021-9517/97 $25.00

Catalyst pretreatment was performed in a fixed-bed reactor by flushing the catalyst with 12.5 ml min^{-1} nitrogen (99.995% N_2, $O_2 < 10$ ppm, $H_2O < 10$ ppm) at 673 K for 30 min followed by a reductive treatment in 30 ml min^{-1} hydrogen (99.999% H_2, $O_2 < 2$ ppm, $N_2 < 3$ ppm, $H_2O < 5$ ppm, $C_nH_m < 0.5$ ppm) for another 90 min. The catalyst was then cooled to room temperature either in hydrogen or in nitrogen and transferred into the autoclave under exclusion of oxygen. The catalyst was first contacted with the solvent containing the proper amount of modifier.

The hydrogenation of KPL was carried out in a 100-ml stainless-steel autoclave (Baskerville) with a 50-ml glass liner and PTFE cover, to provide clean conditions. Under standard conditions, 150 mg pretreated catalyst (cooling in hydrogen after pretreatment), 18 mg HCD, 0.5 g KPL, and 20 ml toluene were used at 70 bar and 285 K. The atmospheric pressure hydrogenations were performed in a 100-ml magnetically mixed glass reactor connected to a glass burette. The reaction was followed by taking samples and analyzing with GC.

Reaction temperatures in figures and tables represent the controlled temperature of the bath into which the autoclave was immersed. The pressure was held at a constant value by computerized constant volume–constant pressure equipment (Büchi BPC 9901). In this system a standard volume of hydrogen is injected when the pressure inside the reactor drops below a preset value. By monitoring the pressure inside the vessel and the injected pulses, the hydrogen uptake can be followed. The reactor was magnetically mixed ($n = 1000$ min^{-1}). It was proved that under standard conditions the rate of hydrogen uptake was independent of the mixing frequency between 500 and 1000 min^{-1}.

ee and conversion were determined with an HP 5890A gas chromatograph with a chiral WCOT cyclodextrin-β-2,3,6-M-19 (Chrompack) capillary column. The enantioselectivity is expressed as ee (%) $= 100 \times (|[R] - [S]|)/([R] + [S])$. ee values were determined at full conversion, if not otherwise stated.

Catalyst samples for transmission electron microscopy (TEM) were suspended into hexane and loaded onto perforated, thin carbon films supported on copper grids. High-resolution TEM was carried out on a Philips CM30ST at 300 kV, with a point resolution of 0.19 nm. Particles were measured from photographic enlargements of the micrographs. The most important parameter obtained from the size distribution is the mean diameter from the surface area-weighted particle size data, $\langle d \rangle_a$ defined by

$$\langle d \rangle_a = \sqrt{\frac{\sum n_i d_i^2}{\sum d_i}}. \qquad [1]$$

CO chemisorption on Pt/alumina was carried out in a Micromeritics ASAP 2000 chemisorption apparatus, at 308 K and a pressure ranging from 0 to 45 kPa. Prior to characterization, the sample was reduced in hydrogen at 673 K for 90 min and evacuated at the same temperature at 10^{-3} Pa for 30 min.

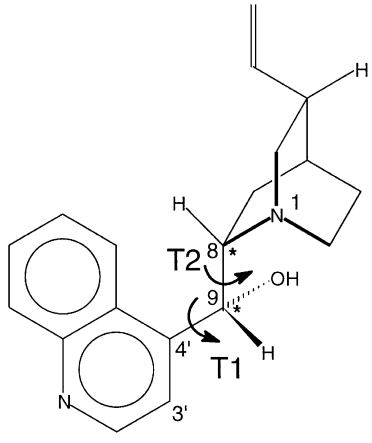

SCHEME 2

Molecular modeling for the conformational analysis of CD (and also the complexes formed between cinchonidine and the reactant) was performed using the MM2 force field as implemented in the HyperChem package (24). The charges of CD atoms were calculated using the AM1 semiempirical molecular orbital method (25). In this analysis all the geometrical parameters of the modifier were optimized without any constraint except the two dihedral angles, T1 and T2 (Scheme 2), which were used as parameters and varied from -180.0° to $+180.0^\circ$ by steps of 10.0°. All the calculations were performed on a PC, applying the default values of the software. The CD conformers were then fully optimized by the *ab initio* method using the 3-21G basis set at the SCF level (26). The Hondo 8.5 program (27) running on an IBM SP2 parallel machine was used for this purpose. As such calculations of the relative energies of conformers of organic systems do not generally need introduction of electron correlation nor the use of extensive basis sets, one can estimate the error bars on such energies as about ± 1 kcal/mol. The same error probably applies to MM2 energies, as the parameters of this force field have been consistently derived so as to perform accurate evaluations of the relative energies of conformers.

RESULTS

Influence of Catalyst Pretreatment

It has been proposed (15) that before the enantioselective hydrogenation of KPL takes place the Pt catalyst should be modified with CD in an ethanolic solution at reflux temperature. This modified 5 wt% Pt/C catalyst provided 36% ee in benzene at 60 bar (15). The application of this procedure under partly different conditions (5 wt% Pt/alumina instead of 5 wt% Pt/C, toluene instead of benzene, and 20 bar instead

TABLE 1

Role of Catalyst Pretreatment and Added Water in the Enantioselective Hydrogenation of Ketopantolactone[a]

Entry	Catalyst pretreatment	H_2 pressure (bar)	[reactant]/ [modifier]	Time (h)	Conversion (%)	ee (%)
1	Reflux in EtOH/CD[b]	60	—	—	—	36
2	Reflux in EtOH/CD	20	240	2	80	21
3	H_2 at 673 K, cooling in N_2	20	240	3	100	56
4	No pretreatment	90	480	1	100	25
5	H_2 at 673 K, cooling in N_2	90	480	1	100	52
6	H_2 at 637 K, cooling in H_2	90	480	1	100	68
7	H_2 at 673 K, cooling in H_2[c]	90	480	1	100	76
8	H_2 at 673 K, cooling in H_2[c,d]	90	480	1	100	40

[a] Reactions were performed in toluene at 285 K using 50 mg of Pt/Al_2O_3.
[b] Solvent: benzene instead of toluene, data taken from Ref. (15).
[c] 156 mg catalyst.
[d] Addition of 2.8 mmol water.

of 60 bar) resulted in only 21% ee (Table 1.) A change of the modifier from CD to HCD had no significant effect on the ee (deviation less than 1%). Besides, there was no detectable variation of ee above 30% conversion.

When searching for reasons of poor enantioselectivity, it must be considered that ethanol is not an inert solvent in carbonyl hydrogenations over Pt (28, 29). Destructive adsorption of ethanol (and other primary alcohols) produces CO- and C_xH_y-type fragments on the Pt surface (29, 30). In addition, ethanol remaining on the catalyst after the pretreatment procedure forms hemiketal from the activated keto group of the reactant. The hemiketal formation is catalyzed by the basic quinuclidine N atom of CD (1, 28).

Accordingly, the catalyst pretreatment in refluxing ethanol was replaced by a prereduction at elevated temperature in flowing hydrogen, a procedure that has been found most suitable for α-ketoester hydrogenation (28). CD was simply added to the catalyst in the solvent used for the hydrogenation reaction. This change in pretreatment conditions resulted in an increase of 35% in ee, under otherwise identical conditions (Table 1, entries 2 and 3). Temperature-programmed oxidation and FTIR analysis of the processes occurring during heat treatment of the catalyst showed that some water, CO_2 (adsorbed on the alumina support), and organic impurities were removed from the surface (31). Removal of surface impurities is one feasible explanation for the enhancement of ee after thermal pretreatment (Table 1).

Another important influence of thermal treatment is indicated by TEM investigation of Pt/alumina before and after heat treatment. As illustrated in Fig. 1, the average particle size increases during thermal treatment at 673 K by ca. 40%, and the calculated dispersion drops from 0.38 to 0.27. For comparison, a platinum dispersion of 0.24 was found with CO chemisorption for the pretreated catalyst. The formation of relatively large, flat crystalline Pt particles, characteristic of the hydrogen-treated catalyst, is favorable for the enantioselectivity, as has been demonstrated previously (3).

An important part of the pretreatment procedure is the cooling of the catalyst after reduction in hydrogen. Cooling

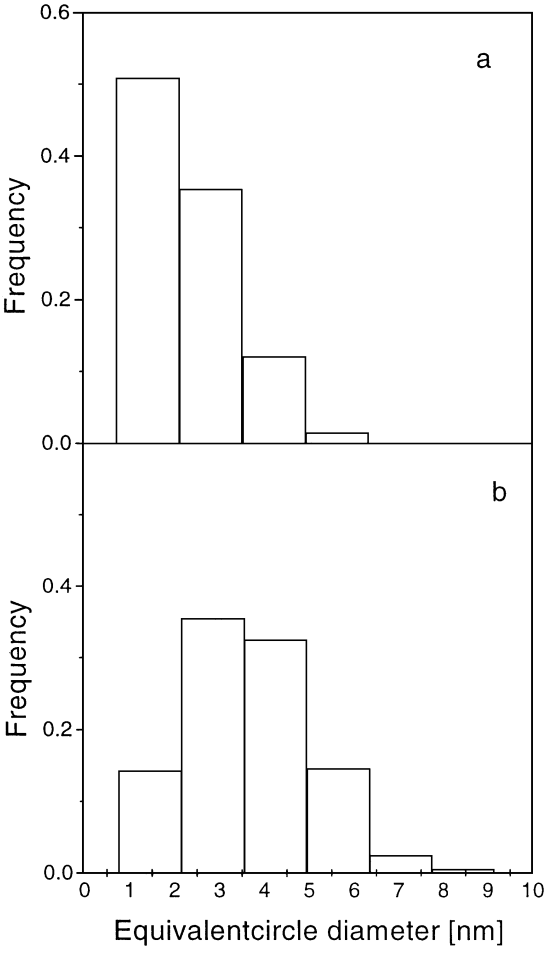

FIG. 1. Frequencies of the equivalent circle diameters calculated from the TEM pictures (a) before and (b) after heat treatment.

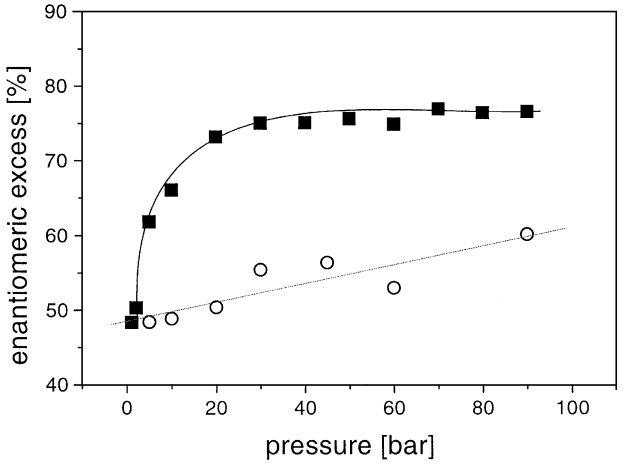

FIG. 2. Influence of pressure on the enantiomeric excess. The catalyst is cooled in hydrogen (■) or nitrogen (○) after heat treatment (150 mg catalyst, 0.067 mmol HCD, 3.9 mmol KPL, 285 K, 70 bar H_2, toluene).

the catalyst in nitrogen lowers the ee (Table 1, entries 5, 6), compared with the ee obtained after cooling in hydrogen. The difference is a function of reaction conditions (hydrogen pressure, amount of catalyst), as can be seen in Figs. 2 and 3. Although this effect is not yet fully understood, a possible explanation of this observation is the chemisorption of oxygen, contained as impurity in N_2 (<10 ppm), and subsequent formation of PtO_x on the Pt surface. After the hydrogenation reaction is started in the autoclave, PtO_x is reduced to Pt^0 and H_2O. Contamination of surface Pt atoms with a submonolayer of water can lower the ee considerably. In a control experiment 50 μl water (0.25 vol% related to the solvent) was added to the reaction mixture and the ee dropped from 76 to 40% (Table 1, entries 7 and 8). Note that the effect was considerably smaller, only 5%, when the catalyst was exposed to air

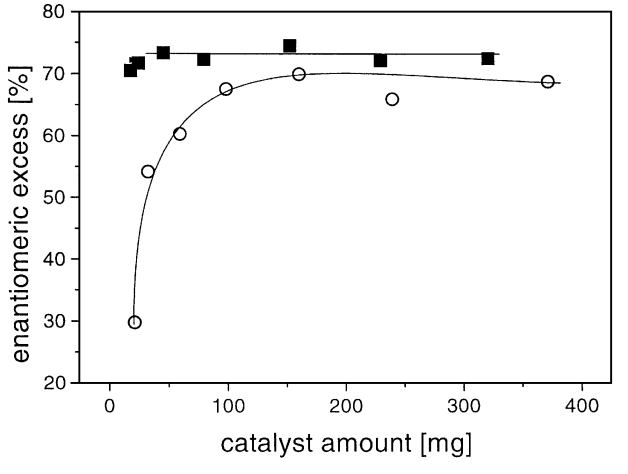

FIG. 3. Influence of catalyst amount on the enantiomeric excess after cooling the catalyst in hydrogen (■) or in nitrogen (○) (catalyst/HCD weight ratio: 7.5, 3.9 mmol ketopantolactone, 285 K, 70 bar H_2, toluene).

at ambient temperature (after heat treatment and cooling in hydrogen).

For comparison, in the general pretreatment procedure applied before the hydrogenation of ethyl pyruvate (8, 28), the catalyst was always cooled after pretreatment in a nitrogen flow. The oxygen contamination of nitrogen had no detectable negative effect on the ee of the reaction. In contrast, stirring the reaction mixture (ethanolic solution) in the presence of air after the heat treatment and before the hydrogenation reaction even increased the ee and the reaction rate (28, 32). The latter effect has been explained partly by the formation of acetic acid from ethanol and subsequent protonation of the quinuclidine nitrogen of CD (28).

Influence of Pressure

There is a considerable enhancement of enantioselectivity with increasing hydrogen pressure, as shown in Fig. 2. Above 40 bar, ee reaches a plateau. This behavior is similar to that observed in the hydrogenation of ethyl pyruvate (2, 32). The relatively high surface hydrogen concentration attainable at high hydrogen pressure seems to be favorable for the enantiodifferentiation. The rate of hydrogen uptake was not influenced by mass transport (hydrogen dissolution and diffusion in the liquid phase) when using 150 mg catalyst at 70 bar pressure. Note that working under standard conditions the reaction rate could not be determined reliably because of the small amount of KPL reactant and, consequently, low hydrogen consumption. A complete kinetic analysis including optimization of the reaction conditions is presently underway.

As discussed above, the ee is considerably lower when the catalyst is cooled in N_2 after heat treatment in H_2 (Fig. 2). In addition, the reproducibility of ee under these conditions is very poor (unusually high standard deviation).

Influence of Catalyst Amount

The role of catalyst amount is shown in Fig. 3. Pt together with HCD modifier is considered the active and selective catalyst system; accordingly, the catalyst/modifier ratio was always kept constant. There is hardly any change in ee with the amount of catalyst when cooling the catalyst in hydrogen after pretreatment. A small drop in selectivity at very low catalyst loading is likely due to experimental difficulties in transferring the prereduced catalyst to the autoclave under exclusion of oxygen, as discussed above. In this region of catalyst loading, ee is extremely low when the catalyst is coold in nitrogen after prereduction at 673 K.

Influence of Solvent

In the hydrogenation of ethyl and methyl pyruvate with cinchonidine-modified Pt, ee decreases with increasing solvent polarity (13, 28, 23). Quite similar behavior is observed in the hydrogenation of KPL, as illustrated in Fig. 4. Good

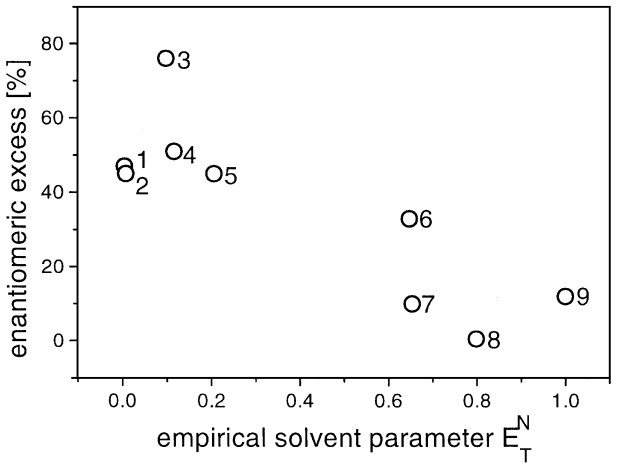

FIG. 4. Influence of the solvent on the enantiomeric excess listed in the order of the empirical solvent parameter, E_T^N (34). The experiments were carried out with 150 mg catalyst, 0.067 mmol modifier, 3.9 mmol ketopantolactone, at 285 K and 70 bar H_2. The solvents are (1) cyclohexane, (2) hexane, (3) toluene, (4) diethyl ether, (5) THF, (6) acetic acid, (7) ethanol, (8) formamide, (9) water.

ee can be obtained only in an apolar medium, such as toluene. In polar solvents, ee drops to zero or close to it. The trend of decreasing enantioselectivity with increasing solvent polarity is even more pronounced than in the case of ethyl pyruvate hydrogenation on Pt/alumina (28). The negative correlation between solvent polarity and ee is not rigorous. For example, in toluene, ee is higher by about 25% than the ee measured in diethyl ether, though the empirical solvent parameters (34) are almost identical for these two solvents. A likely reason for the unexpectedly low ee in the most apolar solvents hexane and cyclohexane is the limited solubility of KPL and CD. In these instances, the reactions were performed in the presence of undissolved KPL. Note that when applying the dielectric constants as values characteristic of solvent polarity, there are also strong deviations from the linear correlation.

No by-products (from side reactions such as acid- or base-catalyzed ring opening and dimerization) could be detected by GC and NMR analysis, when using acetic acid or ethanol as solvents. Nevertheless, by-product formation in small amounts and strong adsorption on the metal surface cannot be excluded. (The detection limit was about 0.5 mol%.)

The influence of solvent polarity may be explained partly by the change in hydrogen solubility with the empirical solvent parameter. There is a general tendency for the solubility of hydrogen to decrease with increasing solvent polarity, independent of pressure (35); however, because of the complex phenomena occurring on the catalyst surface before steady state is achieved (removal of impurities, competitive adsorption of reaction components), a direct relation between hydrogen solubility and enantioselectivity is not apparent (30).

Other possible reasons for the very low ee achieved in polar solvents could be the interaction of solvent with the modifier, resulting in a less favorable conformation (36–38), and the strong adsorption of the solvent molecules on the active sites.

Influence of Modifier

A broad maximum in ee has been observed as a function of modifier concentration (Fig. 5). Interestingly, this maximum corresponds to a rather low HCD/Pt_s (surface Pt atoms) molar ratio of about 0.065. The corresponding cinchona alkaloid/Pt_s molar ratio was found to be 0.5 in the enantioselective hydrogenation of ethyl pyruvate under similar conditions [toluene, 5 wt% Pt/alumina (39)].

When cinchonine, the near enantiomer of CD, was used, (*S*)-pantolactone was formed in excess (ee = 73%).

Influence of Temperature

The enantioselectivity reaches its maximum at around 288 K in toluene at 70 bar, as illustrated in Fig. 6. There is no unambiguous explanation yet for the volcano-type curve. For comparison, in the enantioselective hydrogenation of α-ketoesters, ee increases with decreasing reaction temperature, reaching a plateau below room temperature (2, 32). On the other hand, a maximum in ee as a function of temperature was observed in the enantioselective hydrogenation of pyruvic acid oxime (40).

Influence of Reactant Concentration

Reactant concentration in the range 0.05–2 mmol l^{-1} had only a minor influence on ee, as illustrated in Fig. 7. At low KPL/catalyst ratios, ee decreased by 3%, likely due to the relatively large contribution of the initial transient period (increase in surface hydrogen concentration to the

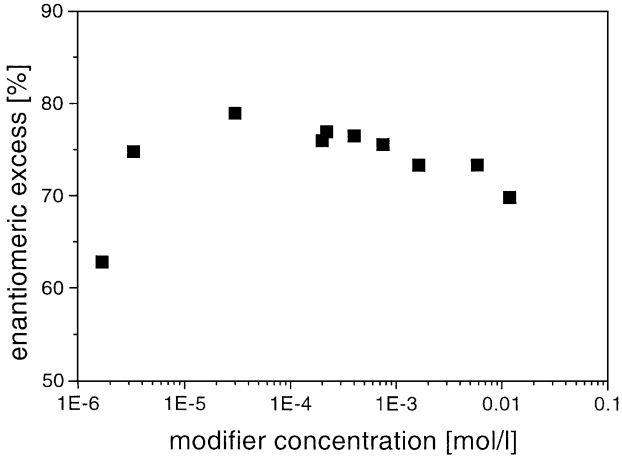

FIG. 5. Influence of modifier (HCD) concentration on the enantiomeric excess (150 mg catalyst, 3.9 mmol ketopantolactone, 285 K, 70 bar H_2, toluene).

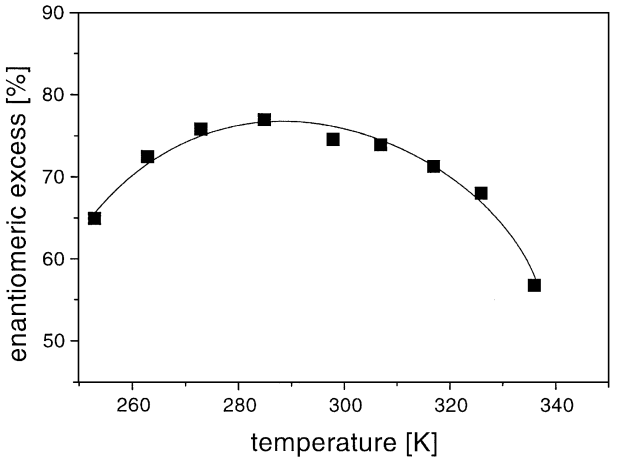

FIG. 6. Influence of temperature on the enantiomeric excess (150 mg catalyst, 0.067 mmol HCD, 3.9 mmol ketopantolactone, 70 bar H_2, toluene).

steady-state value and possible removal of surface impurities by the competitive adsorption of hydrogen; see below).

Influence of Conversion at Atmospheric Pressure

An interesting feature of Pt- and Pd-catalyzed enantioselective hydrogenation of activated carbonyl compounds and olefins, respectively, is that both the ee and the reaction rate increase in the first part of the reaction (6, 30). In contrast, there was no significant change in ee as a function of KPL conversion when the reactor was operated in the kinetic regime. A considerable increase in ee (from 20 to 35% between 5 and 90% conversion) was observed at atmospheric pressure in toluene. In addition, a maximum in reaction rate was obtained at 40–50% conversion; however, these changes were found to be due to the inefficient hydrogen transport in the system. A practically constant ee was measured even at 1 bar, when the influence of mass transport was eliminated. It has recently been shown (30) that

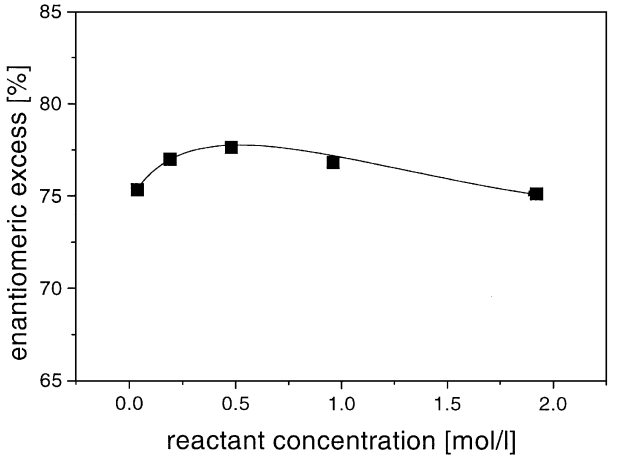

FIG. 7. Influence of reactant concentration on the enantiomeric excess (150 mg catalyst, 0.067 mmol HCD, 285 K, 70 bar H_2, toluene).

the initial transient period during enantioselective hydrogenations over Pt and Pd is due mainly to (i) competitive adsorption of reactant modifier, hydrogen, and solvent and (ii) removal of surface impurities.

Optimization

A limited optimization including the most important reaction parameters (pressure, temperature and amount of modifier) using the gradient method resulted in an ee of 79%. The corresponding conditions are 70 bar and 285 K, using 140 mg 5 wt% Pt/alumina, 3.8 mmol KPL, 0.18 mg HCD, and 20 ml toluene. Remarkable is the very small amount of modifier necessary to obtain high enantioselectivity. It is likely that involvement of other parameters (e.g., catalyst nature, solvent) in the optimization process will provide further improvement in ee.

Rate Acceleration by Cinchona Alkaloids

There is a considerable rate acceleration in the hydrogenation of KPL in the presence of cinchona alkaloids. An example illustrating this "ligand acceleration" effect (39) is shown in Table 2. A relatively high KPL concentration was applied to obtain reliable hydrogen consumption rate data. The initial rate of hydrogen consumption increased by a factor of almost 6 in the presence of HCD. A comparison of modified and racemic reactions is also made based on the overall rate or reaction time. The reaction time necessary for 75% conversion of KPL was found to be seven times lower in the presence of HCD, as compared with the racemic reaction (Table 2). In the enantioselective hydrogenation of ethyl pyruvate over the same catalyst system, the rate acceleration was between 4 and 25 depending on the reaction conditions (2).

Molecular Modeling

The possible mechanism of enantiodifferentiation in the hydrogenation of KPL was studied by theoretical calculations. We focused first on the interaction between the cinchona alkaloid modifier and the activated carbonyl compound reactant, and then on the adsorption of the activated complex. Both molecular mechanics (MM) and *ab initio* calculations were performed to determine the minimum

TABLE 2

Rate Acceleration Observed in the Presence of HCD, at Close to the Optimum Conditions (150 mg Catalyst, 19.5 mmol KPL, 25 ml Toluene, 70 bar, 12°C)

HCD (mg)	ee (%)	r_0 (mmol $h^{-1}(g_{cat})^{-1}$)	$t_{75\%}$[a] (min)
0	—	420	25
20	70	2470	3.5

[a] Reaction time required for 75% KPL conversion.

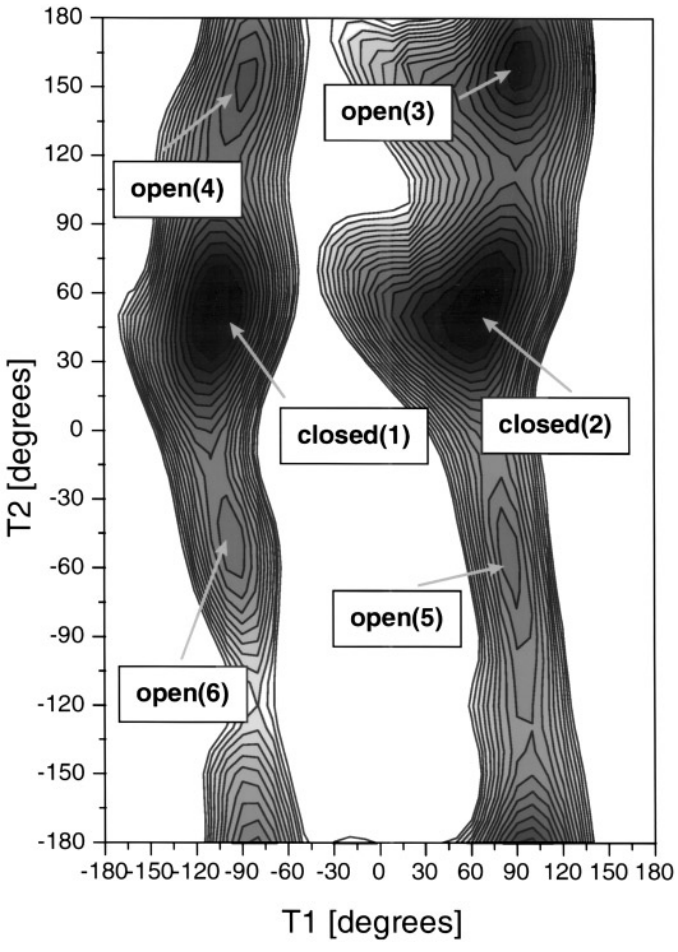

FIG. 8. Isoenergy contour plots calculated (MM) for cinchonidine as a function of the dihedral angles T1 and T2 (show in Scheme 2). The energy spacing between the contours is 0.5 kcal/mol.

energy conformation of CD. It is known from the literature (36–38) that rotations around C4′–C9 and C9–C8 bonds are the most important. The corresponding dihedral angles T1 and T2 are shown in Scheme 2. Isoenergy contour plots calculated (MM) as a function of these dihedral angles are represented in Fig. 8. Six different energy minima (dark area) can be identified as a function of T1 and T2. The numbering of minima 1–4 corresponds to that used by Dijkstra *et al.* (37). In the so-called "closed" conformation the quinuclidine nitrogen is oriented toward the aromatic rings, whereas in the "open" conformation it points away from the aromatic rings. For illustration see also Fig. 9.

It is interesting to compare the results of our *ab initio* calculations with those obtained by Dijkstra *et al.* using one- and two-dimensional NMR techniques, combined with MM and semiempirical molecular orbital calculations (38). According to these methods, the first four minima only were identified; the open(5) and open(6) conformers were not found. It is notheworthy that additional calculations performed by us indicated also six energy minima for cinchonine (CN), the near enantiomer of CD.

The key question is now which of these six minimum energy conformations should be chosen for further calculations. To find the most stable conformer, conformers (1–6) were optimized without constraints; the corresponding relative energies (ΔE) and the dihedral angles T1 and T2 are collected in Table 3. Both *ab initio* and MM calculations indicate that the open(3) conformation is the global minimum. Moreover, this conformer corresponds to that observed by Oleksyn using X-ray crystallography (41). The calculated T1 and T2 dihedral angles are 100.5° and 156.2° (*ab initio*) for open(3) and 101.4° and 158.1° in the X-ray structure.

Figure 9 displays the three-dimensional space-filling models of open(3) and closed(1) conformers. These conformations suggested by *ab initio* calculations were observed in solution by NMR (38). Closed(1) exhibits the lowest energy among the closed conformations, but it is still higher in energy by 3.3 kcal/mol than open(3). It is clearly seen that in the closed(1) conformation the lone electron pair of the quinuclidine N atom points toward the quinoline rings and

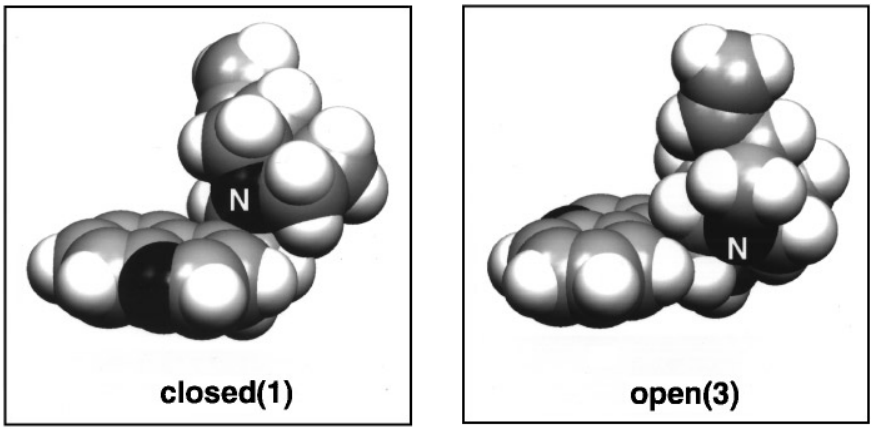

FIG. 9. Space-filling models of the two minimum energy conformations closed(1) and open(3). Colors: H, white; C, gray; O, N, black; white "N" indicates the quinuclidine N atom.

TABLE 3

T1 and T2 Dihedral Angles and the Relative Energies ΔE^a of the Six Conformers of Cinchonidine Fully Optimized Using the Force Field MM2 and the *ab Initio* Method (3–21G Basis Set at the SCF Level)

Conformer	MM2	3–21G
Closed(1)		
T1 (deg)	−106.5	−107.1
T2 (deg)	48.8	54.6
ΔE (kcal/mol)	1.0	3.3
Closed(2)		
T1 (deg)	63.1	70.1
T2 (deg)	45.0	45.7
ΔE (kcal/mol)	1.5	6.4
Open(3)		
T1 (deg)	93.2	100.5
T2 (deg)	156.4	156.2
ΔE (kcal/mol)	0.0	0.0
Open(4)		
T1 (deg)	−96.6	−94.1
T2 (deg)	129.2	137.5
ΔE (kcal/mol)	4.4	3.7
Open(5)		
T1 (deg)	92.7	89.5
T2 (deg)	−82.7	−57.1
ΔE (kca/mol)	3.7	10.1
Open(6)		
T1 (deg)	−95.4	−93.8
T2 (deg)	−59.4	−61.0
ΔE (kcal/mol)	2.0	7.9

[a] ΔE = energy of the conformer related to that of open(3).

it is not accessible to interaction with the carbonyl group of the reactant, adsorbed nearby on the Pt surface. A further support to the choice of open(3) is that this is the preferred conformation in many apolar and protic polar solvents as found by Dijkstra *et al.* (38). These considerations led us to use the open(3) minimum in further calculations.

Application of various derivatives of CD as the source of chiral information in the enantioselective hydrogenation of α-ketoesters indicated that the basic quinuclidine N atom (or its protonated form) is responsible for the interaction with the reactant (13). The successful application of some simple chiral amines as modifiers (8–11) shows that the presence of the 1,2-aminoalcohol structural part in the modifier, characteristic of cinchona alkaloids, is not a prerequisite for achieving high ee. It is very likely that the (C9)−O atom of CD is not involved in the reactant–modifier interaction, but it seems to be important in stabilizing the proper conformer of CD, adsorbed on Pt. Our previous MM calculations (not reported here) questioned the feasibility of the formation of a six-membered ring intermediate involving the quinuclidine N and (C9)−O atoms of CD as electron donors to the carbonyl C atoms of the reactant, as proposed by Augustine *et al.* (5).

It has recently been proposed (42, 43) that one of the closed conformations of CD would interact with the α-ketoester reactant, and the π orbitals of the quinoline ring of CD would stabilize the reactant via π–π overlapping with the conjugated double bond; however, no details of the MM calculations or any data supporting this "specific shielding effect" have been provided by the authors. Moreover, the experimental evidence on which the model was based, namely that ee is close to zero at very low pyruvate conversion, has recently been proved to be erroneous (30).

The structures and energies of complexes formed on interaction of KPL and CD have been calculated by MM (MM2 force field). In these calculations all the geometric parameters have been optimized without any constraint. The atomic charges have been calculated at the semiempirical level using the AM1 method. Figure 10 shows the calculated minimum energy conformations of the CD–KPL adduct leading to the formation of (*R*)- or (*S*)-PL on hydrogenation. In these models, the optimum conformations of the complexes have been accommodated on an ideal Pt(111) "surface," assuming flat adsorption of the aromatic rigs parallel to the Pt surface over two adjacent Pt atoms. This plausible orientation of the modifier has been evidenced by recent adsorption studies using scanning tunneling microscopy for the naphthalene/Pt system (44) and H/D exchange experiments for HCD/Pt system (45).

The top views of the space-filling models of complexes and the corresponding formulas are shown in the lower part of Fig. 10. In the CD–KPL complex the carbonyl O atom of KPL is bound to the quinuclidine N atom of alkaloid via H bonding. The activated complex resembles the half-hydorgenated state of the carbonyl group (late transition state). Note that the stabilization of the half-hydrogenated state of ethyl pyruvate by CD has already been proposed by Wells and co-workers (46). The complex leading to the formation of the (*S*)-product on hydrogenation was found to be energetically less favorable by 2.2 kcal mol^{-1} (Table 4).

For comparison, the same calculations have been performed to determine the nature of the interaction between

TABLE 4

Interaction Energies E_{int} Calculated Using the MM2 Force Field for the Cinchonidine (CD)–Ketopantolactone (KPL), CD–Methyl Pyruvate (MP), and Cinchonine (CN)–MP Interactions[a]

Complex	E_{int} (kcal/mol)		ΔE^b
	Pro (*R*)	Pro (*S*)	
KPL(H)–CD	−20.2	−18.0	2.2
MP(H) (*trans*)–CD	−20.9	−14.3	6.6
MP(H) (*trans*)–CN	−13.4	−20.3	6.9

[a] The transition complexes resemble the half-hydrogenated state of reactants, which is indicated by "H" in brackets.

[b] $|E_{int}(R) - E_{int}(S)|$.

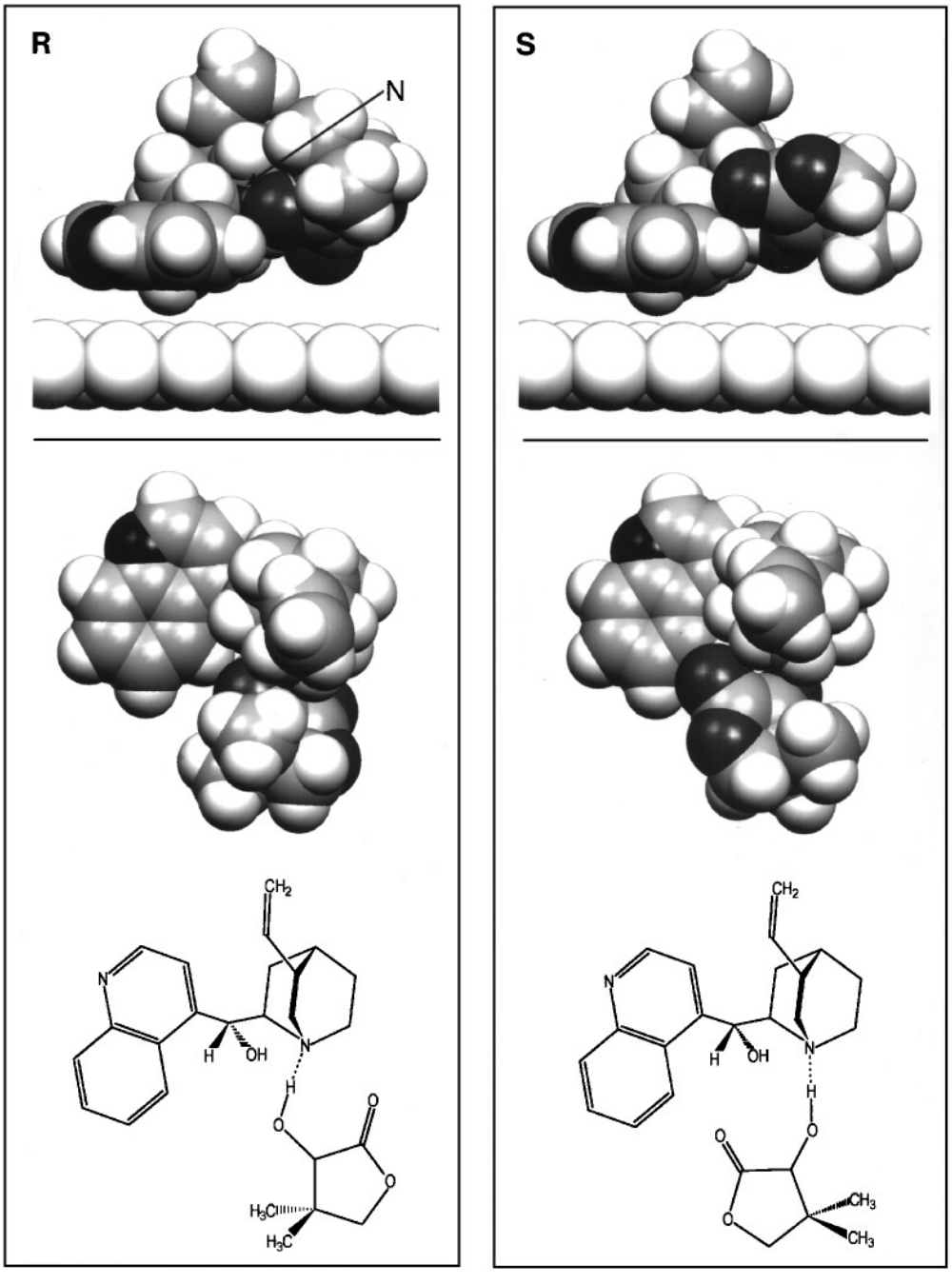

FIG. 10. Space-filling models of the transition complexes formed between CD and ketopantolactone which yield (*R*)- and (*S*)-PL (left and right, respectively). Top: side view over an ideal Pt(111) "surface." Bottom: top view of the space-filling model, together with the formula. Colors as in Fig. 9.

CD and the simplest α-ketoester, methyl pyruvate (MP). The minimum energy conformation of MP was determined by *ab initio* calculations. In the lowest energy state the two carbonyl groups are in *trans* configuration. The calculated minimum energy conformations leading to the formation of (*R*)- and (*S*)-methyl lactates on hydrogenation are depicted in Fig. 11. The space-filling models are accommodated in side views over a schematic Pt surface, assuming that both the aromatic rings of CD and the two carbonyl groups of MP are adsorbed parallel to the flat Pt surface. The calculated interaction energies are collected in Table 4. The formation of (*R*)-lactate is energetically favored when using CD as modifier, but the (*S*)-enantiomer is the preferred product when CN is used in the calculations. The results of these calculations are in agreement with the experimental observations (1, 32).

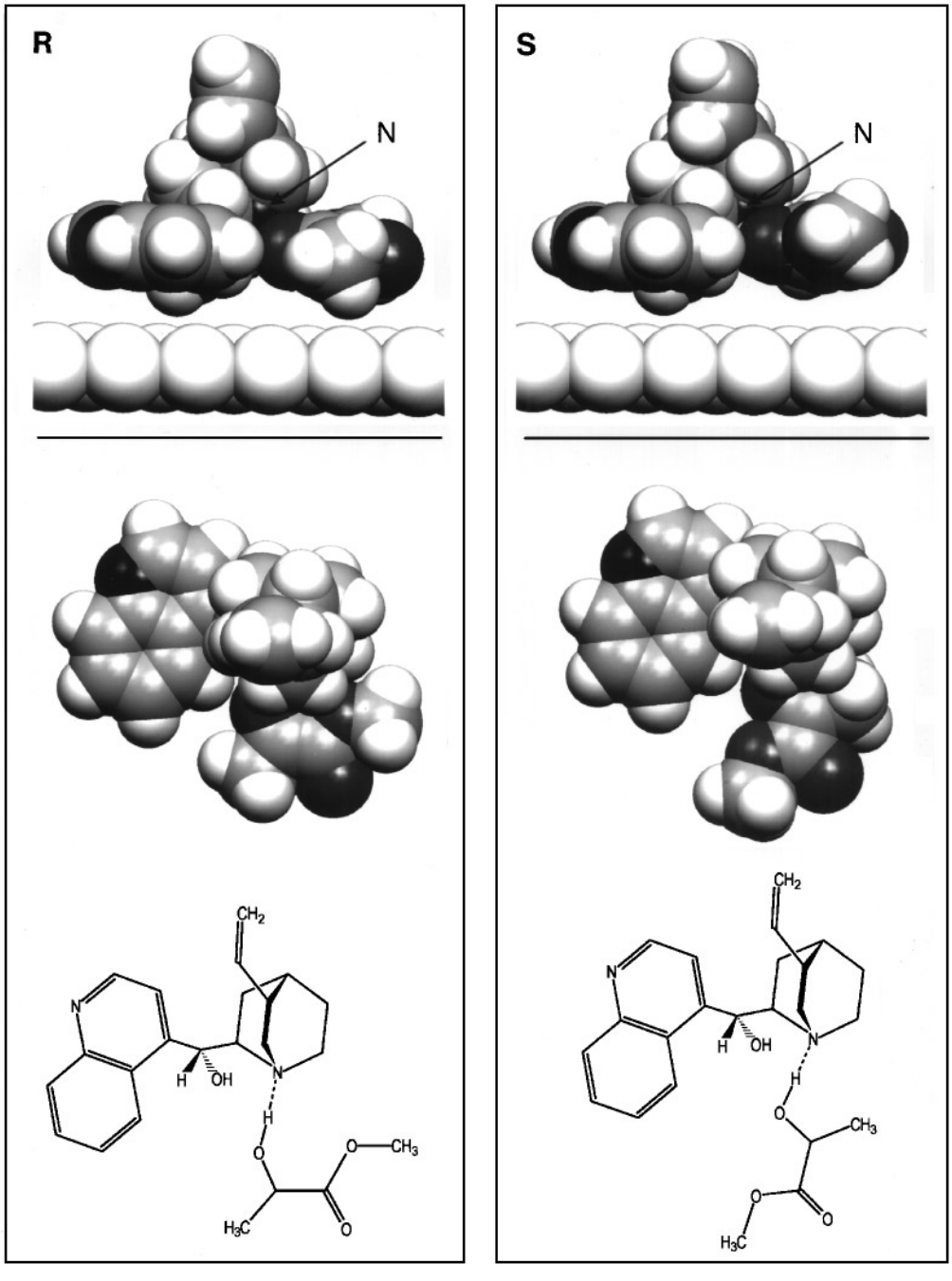

FIG. 11. Space-filling models of the transitions complexes formed between CD and MP which yield (*R*)- and (*S*)-lactate (left and right, respectively) on hydrogenation. Top: side view over an ideal Pt(111) "surface." Bottom: top view of the space-filling model, together with the formula. Colors as in Fig. 9.

DISCUSSION

The enantioselective hydrogenation of the cyclic lactone KPL over cinchona-modified Pt/alumina exhibits characteristics similar to those of the hydrogenation of α-ketoesters. Typical examples are the positive influences of catalyst pretreatment at elevated temperature in flowing hydrogen, the low solvent polarity, and relatively high surface hydrogen concentration on the enantiodifferentiation. An advantageous feature of the reaction is the rather small amount of chiral modifier necessary to induce the maximum ee. The calculated ratio of 1 molecule CD to 15 surface Pt atoms includes the "inefficient" fraction of alkaloid, i.e., the modifier that is adsorbed on the alumina surface or present in the

toluenic solution in steady state. It is very likely that only a minority of surface Pt atoms are covered by CD, even if we consider the relatively large size of active site ensembles covered by one single modifier molecule.

The preliminary optimization of the reaction conditions, involving only a few important parameters, afforded 79% ee in toluene, at below room temperature and high hydrogen pressure. This value corresponds to an increase of 27% compared with the only previous report on the enantioselective reduction of KPL catalyzed by the Pt–CD system. This improvement is attributed to three main reasons:

1. The supported Pt is properly preconditioned before the hydrogenation reaction. Catalyst prereduction at elevated temperature in flowing hydrogen is a simple and efficient way to provide clean, relatively large, and "flat" Pt particles preferable for enantiodifferentiation (3, 12).
2. The use of reactive solvents, such as primary alcohols, diols, and some carbonyl compounds (47), has been avoided. In general, polar solvents including traces of water are detrimental to the enantioselectivity.
3. Rigorously oxygen-free conditions have been applied during catalyst pretreatment and the hydrogenation of KPL.

The second and third points represent interesting deviations from the characteristics of the well-known enantioselective hydrogenation of methyl and ethyl pyruvates.

Molecular modeling calculations provided a feasible explanation for the observed enantiodifferentiation. These calculations suggest that in the transition complex the basic quinuclidine N atom of CD is bound to the carbonyl group of KPL via a hydrogen bond interaction (N–H–O connection), stabilizing the half-hydrogenated state of the reactant (46). Because of this interaction, the formation of (*R*)-pantolactone is energetically favored compared with that of (*S*)-pantolactone. When applied to CN, the calculations indicate the preferential formation of the (*S*)-product, in agreement with the experimental observations.

Note that these calculations take into account only the reactant–chiral modifier interaction. Future studies should include the important role of the adsorption bonds of the diastereomeric transition complex. In the present calculation we made the simplifiying assumption that the transition complex adsorbs on Pt in a position that the quinoline rings of CD and the carbonyl groups of KPL are adsorbed parallel to a flat (ideal) Pt(111) surface. The interaction between the solvent and the transition complex, which has not been considered, is likely to be less important in an apolar medium.

The calculations have been extended to the more studied α-ketoester hydrogenation reaction (pyuvate $\rightarrow$ lactate). The *ab initio* and MM calculations demonstrated the similarity of the diastereomeric transition complex when comparing the enantioselective hydrogenation of the cyclic lactone and the α-ketoester in an apolar medium, where the alkaloid is not protonated (39).

The hydrogenation of pyruvate esters provides the highest ee when the CD modifier is protonated (13, 28). For this case we have already proposed a model for the enantiodifferentiation based on molecular modeling calculations (48, 49). When the protonated CD interacts with the activated carbonyl compound the crucial interaction can again be described as a hydrogen bonding between the quinuclidine N atom and the α-carbonyl O atom.

CONCLUSIONS

The present study demonstrates that the hydrogenation of ketopantolactone to (*R*)- or (*S*)-pantolactone can be performed with good enantioselectivity over cinchonidine- or cinchonine-modified Pt/alumina, respectively, provided the catalyst is properly preconditioned and traces of oxygen and water are rigorously removed. It is likely that involvement of a broader range of reaction parameters in the optimization will result in even higher ee's, similar to those characteristic of α-ketoester hydrogenation over cinchona-modified Pt catalysts. Molecular modeling of the diastereomeric transition complexes formed between ketopantolactone and the modifiers cinchonidine and cinchonine indicated that the complex affording (*R*)-pantolactone is energetically favored with cinchonidine, whereas the near enantiomer cinchonine favors (*S*)-pantolactone formation. The structures of these transition complexes are strikingly similar to those calculated for the interaction of these modifiers with methyl pyruvate, the crucial interaction being the hydrogen bonding between the quinuclidine nitrogen of the modifier and the oxygen at the α-carbonyl group of the reactant. Thus, the theoretical studies extend the previous models suggested for the cinchona alkaloid–pyruvate interaction (48), where the modifier exists in protonated form.

ACKNOWLEDGMENTS

Financial support of this work by the Swiss National Science Foundation (Program CHiral 2) is gratefully acknowledged. Thanks are also due R. Wessicken (Department of Solid State Physics, ETH, Zürich) for the electron microscopic measurements.

REFERENCES

1. Orito, Y., Imai, S., and Niwa, S., *J. Chem. Soc. Japan* **8**, 1118 (1979).
2. Blaser, H. U., Jalett, H. P., Monti, D. M., Reber, J. F., and Wehrli, J. T., *Stud. Surf. Sci. Catal.* **41**, 153 (1988).
3. Wehrli, J. T., Baiker, A., Monti, D. M., and Blaser, H. U., *J. Mol. Catal.* **49**, 195 (1989).
4. Sutherland, I. M., Ibbotson, A., Moyes, R. B., and Wells, P. B., *J. Catal.* **125**, 77 (1990).
5. Augustine, R. L., Tanielyan, S. K., and Doyle, L. K., *Tetrahedron Asym.* **4**, 1803 (1993).
6. Singh, U. K., Landau, R. N., Yongkui, S., LeBlond, C., Blackmond, D. G., Tanielyan, S. K., and Augustine, R. L., *J. Catal.* **154**, 91 (1995).

7. Tungler, A., Mathe, T., Fodor, K., Sheldon, R. A., and Gallezot, P., *J. Mol. Catal. A* **108**, 145 (1996).
8. Heinz, T., Wang, G., Pfalz, A., Minder, B., Schürch, M., Mallat, T., and Baiker, A., *J. Chem. Soc. Chem. Common.*, 1421 (1995).
9. Wang, G., Heinz, T., Pfaltz, A., Minder, B., Mallat, T., and Baiker, A., *J. Chem. Soc. Chem. Commun.*, 2047 (1994).
10. Minder, B., Schürch, M., Mallat, T., Baiker, A., Heinz, T., and Pfaltz, A., *J. Catal.* **160**, 261 (1996).
11. Baiker, A., *J. Mol. Catal. A: Chemical* **115**, 473 (1997).
12. Orito, Y., Imai, S., Niwa, S., and Nguyen-Gia-Hung, *J. Synth. Org. Chem. Japan* **37**, 173 (1979).
13. Blaser, H. U., Jalett, H. P., and Wiehl, J., *J. Mol. Catal.* **68**, 215 (1991).
14. Schmid, R., *Chimia* **50**, 110 (1996).
15. Niwa, S., Imamura, Y., and Otsuka, *Jpn. Kokai Tokkyo Koho* **62**, 158268 (1987); *Chem. Abstr.* **109**, 128815f (1988).
16. Carpentier, J.-F., Agbossou, F., and Mortreux, A., *Tetrahedron Asym.* **6**, 39 (1995).
17. Genêt, J. P., Pinel, C., Ratovelomanana-Vidal, Mallart, S., Pfister, X., Bischoff, L., Caño De Andrade, M. C., Darses, S., Galopin, C., and Laffitte, J. A., *Tetrahedron Asym.* **5**, 675 (1994).
18. Hapiot, F., Agbossou, F., and Mortreux, A., *Tetrahedron Asym.* **5**, 515 (1994).
19. Ojima, I., and Kogure, T., *J. Organomet. Chem.* **195**, 239 (1980).
20. Roucoux, A., Devocelle, M., Carpentier, J.-F., Agbossou, F., and Mortreux, A., *Synlett* **4**, 358 (1995).
21. Takahashi, H., Hattori, M., Chiba, M., Morimoto, T., and Achiwa, K., *Tetrahedron Lett.* **27**, 4477 (1986).
22. Roucoux, A., Suisse, I., Devocelle, M., Carpentier, J.-F., Agbossou, F., and Mortreux, A., *Tetrahedron Asym.* **7**, 379 (1996).
23. Mallat, T., and Petró, J., *React. Kinet. Catal. Lett.* **11**, 307 (1979).
24. HyperChem 4.0, Hypercube Inc., 419 Philips Street, Waterloo, Ontario, Canada N2L 3X2 (1994).
25. Dewar, M. J. S., Zoebisch, E. G., Healy, E. F., and Stewart, J. J. P., *J. Am. Chem. Soc.* **107**, 3902 (1985).
26. Binkley, J. S., Pople, J. A., and Hehre, W., *J. Am. Chem. Soc.* **102**, 939 (1980).
27. Dupuis, M., Johnston, F., and Marquez, A., IBM Co., Neighborhood Road, Kingston, NY, 1994.
28. Minder, B., Mallat, T., Skrabal, P., and Baiker, A., *Catal. Lett.* **29**, 115 (1994).
29. Iwasita, T., and Nart, F. C., *in* "Advances in Electrochemical Science and Engineering" (H. Gerischer and C. W. Tobias, Eds.), Vol. 4, p. 123. VCH, Weinheim/New York, 1995.
30. Mallat, T., Bodnar, Z., Minder, B., Borszeky, K., and Baiker, A., *J. Catal.* **168**, 183 (1997).
31. Blaser, H. U., Jalett, H. P., Monti, D. M., and Wehrli, J. T., *Appl. Catal.* **52**, 19 (1989).
32. Meheux, P. A., Ibbotson, A., and Wells, P. B., *J. Catal.* **128**, 387 (1991).
33. Wehrli, J. T., Baiker, A., Monti, D. M., Blaser, H. U., and Jalett, H. P., *J. Mol. Catal.* **57**, 245 (1989).
34. Reichardt, C., *in* "Solvents and Solvent Effects in Organic Chemistry" (H. F. Ebel, Ed.), p. 359. VCH, Weinheim/New York, 1988.
35. Young, C. L., "Solubility Data Series." Pergamon Press, Oxford, 1981.
36. Dijkstra, G. D. H., Kellogg, R. M., Wynberg, H., Svendsen, J. S., Marko, I., and Sharpless, K. B., *J. Am. Chem. Soc.* **111**, 8069 (1989).
37. Dijkstra, G. D. H., Kellogg, R. M., and Wynberg, H., *Recl. Trav. Chim. Pays-Bas* **108**, 195 (1989).
38. Dijkstra, G. D. J., Kellogg, R. M., and Wynberg, H., *J. Org. Chem.* **55**, 6121 (1990).
39. Garland, M., and Blaser, H. U., *J. Am. Chem. Soc.* **112**, 7048 (1990).
40. Borszeky, K., Mallat, T., Aeschimann, R., Schweizer, W. B., and Baiker, A., *J. Catal.* **161**, 451 (1996).
41. Oleksyn, B. J., *Acta Crystallogr. Sect. B* **38**, 1832 (1982).
42. Margitfalvi, J. L., and Hegedüs, M., *J. Mol. Catal.* **107**, 281 (1996).
43. Margitfalvi, J. L., Hegedüs, M., and First, E. T., *Tetrahedron Asym.* **7**, 571 (1996).
44. Hallmark, V. M., and Chiang, S., *Surf. Sci.* **286**, 190 (1993).
45. Bond, G., and Wells, P. B., *J. Catal.* **150**, 329 (1994).
46. Bond, G., Meheux, P. A., Ibbotson, A., and Wells, P. B., *Catal. Today* **10**, 371 (1991).
47. Leung, L.-W. H., and Weaver, M. J., *Langmuir* **6**, 323 (1990).
48. Schwalm, O., Minder, B., Weber, J., and Baiker, A., *Catal. Lett.* **23**, 271 (1994).
49. Schwalm, O., Weber, J., Minder, B., and Baiker, A., *Int. J. Quantum Chem.* **52**, 191 (1994).